NASA TN D-38

TECHNICAL NOTE
D-38

EFFECT OF CHORDWISE HEAT CONDUCTION ON THE TORSIONAL STIFFNESS OF A DIAMOND-SHAPED WING SUBJECTED TO A CONSTANT HEAT INPUT

By Robert G. Thomson and J. Lyell Sanders, Jr.

Langley Research Center
Langley Field, Va.

NATIONAL AERONAUTICS AND SPACE ADMINISTRATION

WASHINGTON

September 1959

NATIONAL AERONAUTICS AND SPACE ADMINISTRATION

TECHNICAL NOTE D-38

EFFECT OF CHORDWISE HEAT CONDUCTION ON THE TORSIONAL STIFFNESS OF A DIAMOND-SHAPED WING SUBJECTED TO A CONSTANT HEAT INPUT

By Robert G. Thomson and J. Lyell Sanders, Jr.

SUMMARY

The effect of thermal stresses in reducing the torsional stiffness of a diamond-shaped wing subjected to a suddenly applied constant heat input is investigated, chordwise heat conduction being taken into account. Analytic solutions are obtained by using separation of variables and Mellin transforms and computed results are given in graphical form. The effect of chordwise heat conduction in reducing the temperature gradients is greatest, as would be expected, near the leading and trailing edges of the wing. The dependence of torsional stiffness reduction on the heating rate and the final wing temperature is inferred from the results obtained.

INTRODUCTION

The influence of chordwise heat conduction has previously been neglected in calculating the effects of aerodynamic heating on the torsional stiffness of thin, solid, diamond-shaped wings. (See, for example, ref. 1.) Because of the neglect of chordwise heat flow, under conditions where heat is applied abruptly the temperature at the leading and trailing edges of the wing instantaneously becomes the final equilibrium temperature and produces a more severe temperature gradient than would actually occur in the structure. The resulting torsional stiffness reduction calculated from this temperature gradient will be of greater magnitude than is actually present.

Related problems in which chordwise heat conduction was considered have been investigated in references 2 and 3. In reference 2 the effect of chordwise heat conduction on the leading-edge temperature of a flat plate subjected to aerodynamic heating is presented. An analysis of the temperature distribution in a diamond-shaped wing subjected to a constant heat input with heat flow permitted along the chord and through the

thickness of the wing is given in reference 3. Neither of these investigations, however, consider the effects of chordwise heat conduction on torsional stiffness.

In the present paper the influence of chordwise heat conduction on the torsional stiffness of a diamond-shaped wing subjected to a constant, uniform, heat input is investigated. Although this heat input is far from that occurring in an actual structure undergoing aerodynamic heating, such a heat input would be realized from suddenly applied radiant heating, as by heating lamps in the laboratory, or from a nuclear explosion. In particular, the assumption of a constant heat input permits an exact analytical solution of this problem. This exact solution can serve two purposes: First, the influence of chordwise heat conduction on torsional stiffness can be quantitatively shown. Second, the exact solution can serve as a basis for the evaluation of approximate procedures that must be applied to obtain the influence of chordwise heat conduction when a structure undergoes aerodynamic heating.

L 3 4 0

SYMBOLS

a	arbitrary constant
A	cross-sectional area, arbitrary constant
$b = 2t_m/c$	
c	chord length
c_n	arbitrary constants ($n = 1, 2, 3, \ldots$)
c_p	specific heat of wing material
D_n	constant defined after eq. (6)
E	Young's modulus
$f(s)$	Mellin transform
G	shear modulus
J	torsional stiffness constant
J_n	Bessel function of the first kind of order n
K	thermal conductivity of wing material

q	rate of heat input per unit area of surface (constant and uniform)
$\mathbf{S}_n$	Struve function of order n
t	wing thickness (bx)
t_m	maximum wing thickness
$\overline{U}$	temperature
U	nondimensional temperature parameter, $\frac{Kb}{qc}\overline{U}$
U_1	nondimensional transient temperature parameter
U_{qs}	nondimensional quasi-steady-state temperature parameter
$V = \frac{U}{\sqrt{\tau_1}}$	
x	distance along chord measured from leading edge
$x_1 = \frac{2x}{c}$	
Y_n	Bessel function of second kind (Weber function) of order n
Z_n	characteristic roots of $J_1(Z_n) = 0$
α	linear coefficient of thermal expansion
ρ	weight density of wing material
τ	time
τ_1	nondimensional time parameter, $\frac{8\eta\tau}{c^2}$
$q\psi(\tau_1)$	torsional stiffness reduction parameter (see eq. (15))
$\xi = \frac{x_1}{\sqrt{\tau_1}}$	
σ	spanwise stress

η thermal diffusivity, $\frac{K}{\rho c_p}$

$\Delta GJ = \frac{(GJ)_0 - (GJ)_{eff}}{(GJ)_0}$

Γ gamma function

Subscripts:

eff effective

el elementary

0 initial

n,m integers

Superscript:

j integer

Primes denote differentiation with respect to x_1 and dots denote differentiation with respect to τ_1.

EFFECTS OF CHORDWISE HEAT CONDUCTION

Temperature Distribution

The analysis of the chordwise temperature distribution in a diamond-shaped wing subjected to a constant heat input is presented in appendix A. In this analysis the spanwise heat conduction was neglected, the temperature through the thickness of the wing was assumed to be constant, and all material properties were considered to be invariant with temperature.

From a consideration of the heat balance in an element of the wing (as shown in fig. 1) the following partial differential equation was obtained after terms of higher order were neglected

$$\rho c_p b x \frac{\partial \bar{U}}{\partial \tau} = 2q + K \frac{\partial}{\partial x}\left(t \frac{\partial \bar{U}}{\partial x}\right) \qquad (1)$$

Equation (1) can be written in nondimensional form as follows:

$$2x_1\dot{U} = 1 + \left(x_1U'\right)' \tag{2}$$

where

$$U = \frac{Kb}{qc}\,\bar{U}$$

$$\tau_1 = \frac{8\eta}{c^2}\,\tau$$

$$x_1 = \frac{2x}{c}$$

The primes denote differentiation with respect to x_1 and the dots denote differentiation with respect to τ_1.

Because of the symmetry of the cross section only half of the chord length was considered. Thus the appropriate boundary conditions were taken to be

$$x_1U' \to 0 \qquad \left(x_1 \to 0\right) \tag{3}$$

$$U'\left(1,\tau_1\right) = 0 \tag{4}$$

with the initial condition taken as

$$U\left(x_1,0\right) = 0 \tag{5}$$

In order to facilitate numerical calculations it was found advisable to make two solutions of the partial differential equation given in equation (2); one solution appropriate for large values of τ_1, and another for small values of τ_1. These solutions are discussed in appendixes A and B.

Long-time solution.- In appendix A the temperature distribution in the wing was found by considering the temperature to be the sum of two parts: a quasi-steady-state solution in which the chordwise temperature distribution is stabilized, and a transient temperature distribution which is a function of both time and position. The final temperature distribution as derived in appendix A is

$$U = \frac{x_1^2}{2} - x_1 + \tau_1 + \frac{5}{12} + \sum_{n=1,2,3,\ldots}^{\infty} D_n J_0(Z_n x_1) e^{-\frac{Z_n^2}{2}\tau_1} \qquad (6)$$

where

$$D_n = \frac{-2}{Z_n^2} \frac{\int_0^1 J_0(Z_n x_1)\,dx_1}{J_0^2(Z_n)}$$

and Z_n is the value that satisfies the equation

$$J_1(Z_n) = 0 \qquad (7)$$

The evaluation of $\int_0^1 J_0(Z_n x_1)\,dx_1$ is described in appendix C.

The chordwise temperature distribution given by equation (6) is identical to the expression for an average (through the thickness) chordwise temperature distribution found in reference 3 where the heat conduction through the thickness and along the chord was considered. Furthermore, as can be seen from figures 7 and 8 of reference 3 only a slight temperature gradient through the thickness of the wing was present.

Theoretically, equation (6) gives the temperature at any station of the cross section at any time. However, for both τ_1 and x_1 small (a short time after the application of heat with attention confined to the vicinity of the leading or trailing edge), a prohibitive number of terms of the series in equation (6) is required to obtain reasonable accuracy. On account of this limitation, equation (6) is referred to herein as the "long-time" solution. Note that for very long times $(\tau_1 > 1)$ the series in equation (6) becomes negligible and continued heating only causes a uniform increase in temperature as a linear function of time. This is referred to as the quasi-steady-state condition.

Since equation (6) could not be practically used for small τ_1 and x_1, a separate "short-time" solution was obtained by a different approach. This approach is briefly described below.

Short-time solution.- For short times $(\tau_1 < 0.01)$ the important happenings are confined to the leading and trailing edges of the wing. Therefore, a solution for the temperature distribution of an infinite

wedge with apex at $x_1 = 0$ was used in appendix A to approximate the short-time temperature distribution in the diamond-shaped wing. The differential equation and boundary conditions were identical to those stated in equations (2) to (5) with the exception of the boundary condition at the midchord (eq. (4)), which is replaced by $U(x_1,\tau_1) \to 0$ as $x_1 \to \infty$.

The character of the "short-time" problem suggested the use of Mellin transforms for its analysis and yielded either an asymptotic or a convergent power series solution. The details of the analysis are given in appendix A.

As shown in appendix A, the short-time temperature distribution for the vicinity of the leading edge and for short-time intervals can best be represented by the convergent power series given as

$$U = \sqrt{\frac{\pi}{2}\tau_1} - x_1 - x_1\sqrt{2\pi}\sum_{n=1,2,3,\ldots}^{\infty} \frac{(-1)^n n(2n-2)!}{2^{3n}(n!)^3}\left(\frac{x_1}{\sqrt{\tau_1}}\right)^{2n-1} \tag{8}$$

For short time intervals excluding the vicinity of the leading edge the asymptotic power series is the more appropriate and is given as

$$U \approx \sqrt{\tau_1}\sum_{m=0,1,2,\ldots}^{\infty} \frac{[(2m)!]^2}{2^{3m+1}(m+1)(m!)^3}\left(\frac{x_1}{\sqrt{\tau_1}}\right)^{-(2m+1)} \tag{9}$$

Elementary solution.- In order to provide a basis for assessing the effect of chordwise heat conduction on the average chordwise temperature distribution, the solution for zero chordwise heat conduction is required. For this case, the thermal conductivity K of the wing material is taken to be zero in equation (1); the following simple relation results:

$$\frac{\partial \bar{U}_{el}}{\partial \tau} = \frac{2q}{\rho c_p b x} \tag{10}$$

By integrating this expression between the initial and final conditions and applying the initial condition $\bar{U}(x_1,0) = 0$, equation (10) becomes

$$\bar{U}_{el} = \frac{2q}{\rho c_p b x} \tau \tag{11}$$

or in nondimensional form

$$U_{el} = \frac{\tau_1}{2x_1} \tag{12}$$

This approximate (or elementary) temperature distribution does not satisfy the additional boundary conditions stated in equations (3) and (4). When x approaches zero, the temperature approaches infinity. At $x = c/2$, the temperature gradient is not zero and a point of discontinuity exists. The inclusion of chordwise heat conduction has therefore reduced the temperature of the leading (and trailing) edge to a finite value and diminished the temperature gradient at the midchord to zero.

L
3
4
0

Results of Temperature Distribution Analysis

In order to show the effect of chordwise heat conduction on the chordwise temperature distribution, the solutions for the temperature distribution with and without chordwise heat flow were plotted across the half-chord in figures 2 and 3.

In figure 2 the ratio of U to U_{el} is plotted across the half-chord for various values of τ_1. In the vicinity of the leading edge $\left(0 < x_1 < 0.1\right)$ equation (8) was used to calculate the temperatures for $0 < \tau_1 < 0.01$. The temperature distribution for the remaining ranges of x_1 and τ_1 was calculated by using equation (6). Note that in the limit as $\tau_1 \to \infty$ in equation (6), $\frac{U}{U_{el}} \to 2x_1$.

In figure 3, U and U_{el} are plotted across the half-chord for various values of τ_1. The influence of chordwise heat conduction can be seen to have the greatest effect, as would be expected, near the leading edge of the wing. In the calculation of torsional stiffness reduction, the temperatures in the vicinity of the leading edge are most important.

Torsional Stiffness Reduction

The presence of chordwise thermal gradients in a cross section induces thermal stresses which in turn cause a reduction in the torsional stiffness of the wing as shown in reference 1. In reference 1 the effective torsional stiffness of a thin wing subjected to spanwise normal stresses was derived and is

$$(GJ)_{eff} = (GJ)_0 + \int_A \sigma\left(\frac{c}{2} - x\right)^2 dA \tag{13}$$

where

$(GJ)_0$ initial torsional stiffness

σ spanwise normal stress (tension positive)

For the diamond-shaped profile (ref. 1), $(GJ)_0 = \frac{1}{12} G c t_m^3$.

For the constant heat input and double symmetry of the wing considered in this paper, the induced thermal stresses will produce only a net average translation of the cross section. (See ref. 4.) The average spanwise strain is therefore a constant and, by application of the equilibrium condition of zero thrust, the spanwise stress can be expressed through

$$\frac{\sigma}{E\alpha} = \frac{\int_A \bar{U}\, dA}{\int_A dA} - \bar{U} \tag{14}$$

The chordwise temperature distribution $\bar{U}$ was derived for long- and short-time conditions; thus, the evaluation of the reduction in torsional stiffness must necessarily be separated in the same way. The following sections deal with the evaluation of torsional stiffness reductions due to these temperature distributions derived for long- and short-time intervals and for the elementary solution in which heat conduction was neglected.

Long-time solution.- Substitution of equation (6) into equation (14) for spanwise stress and taking $(GJ)_0 = \frac{G c t_m^3}{12}$ yields after integration and simplification the expression

$$\frac{(GJ)_{eff}}{(GJ)_0} = 1 - \frac{E\alpha}{G}\left(\frac{c}{t_m}\right)^3 \frac{c}{2K}\left[q\psi(\tau_1)\right] \tag{15}$$

where the torsional stiffness reduction parameter $\left[q\psi(\tau_1)\right]$ is expressed as

$$q\psi(\tau_1) = q\left[\frac{7}{240} + 6\sum_{n=1,2,3,\ldots}^{\infty} D_n \frac{e^{-\frac{Z_n^2}{2}\tau_1}}{Z_n^2}\int_0^1 J_0(Z_n x_1)\,dx_1\right] \tag{16}$$

L 3 4 0

Only the inclusion of the first four terms of the series in equation (16) is necessary to give the effective torsional stiffness within 1 percent for $\tau_1 > 0.01$; for $\tau_1 > 0.08$ only the first term is necessary. The series of Bessel functions was therefore used to calculate the reduction in torsional stiffness for $\tau_1 > 0.01$.

Short-time solution.- For short times ($\tau_1 < 0.01$) the expressions for U given by equations (8) and (9) may be substituted into equation (14) for spanwise stress. In order to evaluate the integrals, however, the temperature distribution was rewritten in the form given by equation (A15) as

$$\bar{U} = \frac{qc}{Kb}\sqrt{\tau_1}\,V\left(\frac{x_1}{\sqrt{\tau_1}}\right) \tag{17}$$

Substitution of equation (17) for $\bar{U}$ into equation (14) for spanwise stress yields

$$\frac{\sigma}{E\alpha} = \frac{qc}{Kb}\left[2\int_0^1 x_1 V\left(\frac{x_1}{\sqrt{\tau_1}}\right)dx_1 - \bar{U}\right] \tag{18}$$

The torsional stiffness reduction parameter (see eq. (15)) therefore becomes

$$q\psi(\tau_1) = q\left[\frac{5\sqrt{\tau_1}}{2}\int_0^1 x_1 V\left(\frac{x_1}{\sqrt{\tau_1}}\right)dx_1 - 6\sqrt{\tau_1}\int_0^1 x_1^2 V\left(\frac{x_1}{\sqrt{\tau_1}}\right)dx_1 + 3\sqrt{\tau_1}\int_0^1 x_1^3 V\left(\frac{x_1}{\sqrt{\tau_1}}\right)dx_1\right] \tag{19}$$

The details for the evaluation of the integrals in equation (19) are given in appendix B. Substitution of these values for the integrals into equation (19) and simplification yields the final expression for the torsional stiffness reduction parameter as

$$q\psi(\tau_1) = q\left[\frac{\tau_1}{4} + \tau_1^2 - \frac{3}{8}\gamma\tau_1^2 - \frac{9}{8}\tau_1^2\log_e 2 - \frac{3}{4}\tau_1^2\log_e\frac{1}{\sqrt{\tau_1}} + \frac{\sqrt{\tau_1}}{2}\sum_{n=2,3,4\ldots}^{\infty}\frac{\left(4n^2 - 10n - 6\right)\left[(2n)!\right]^2\tau_1^{n+1/2}}{(2n-1)(2n-2)(2n-3)2^{3n+1}(n+1)(n!)^3}\right] \tag{20}$$

where $\gamma = 0.5772157\ldots$ Euler's constant.

Elementary solution.- In order to obtain, for the sake of comparison, torsional stiffness reduction without chordwise heat flow the expression for $\bar{U}$ given by equation (11) is substituted into equation (14) for spanwise stress. Thus

$$\frac{\sigma}{E\alpha} = \bar{U}_{el}\left(\frac{2t}{t_m} - 1\right) \tag{21}$$

Substitution of equation (21) into equation (13) for effective torsional stiffness yields, after integration and simplification, the following expression for the torsional stiffness reduction parameter

$$q\psi(\tau_1) = q\frac{\tau_1}{4} \tag{22}$$

Results of Torsional Stiffness Analysis

In order to determine the effect of chordwise heat conduction on the torsional stiffness reduction, the function $\psi(\tau_1)$ was evaluated for various values of τ_1 for the solutions with and without chordwise heat conduction. The results are presented in figure 4 where $\psi(\tau_1)$ is plotted as a function of τ_1. When τ_1 approaches infinity, $\psi(\tau_1)$ without chordwise heat conduction approaches infinity but the solution with chordwise heat conduction approaches asymptotically the value $\frac{7}{240} = 0.0292$. (See eq. (16).) Thus the torsional stiffness reduction with chordwise heat conduction levels off after a finite reduction.

L 3 4 0

For the solution involving chordwise heat conduction the short-time solution was used for $\tau_1 < 0.01$ and the series part of equation (20) was found to be negligible. For $\tau_1 > 0.01$ the long-time solution given by equation (16) was used and required only two to three terms in the series to obtain accuracy within 1 percent. As τ_1 increases, the number of necessary terms in the series of equation (16) decreases until for $\tau_1 > 0.08$ only the first term was needed for accuracy within 1 percent.

A more useful and convenient presentation of the results of figure 4 might be effected if the influence of chordwise heat conduction on the reduction in torsional stiffness is related to the magnitude of q/K the ratio of heating rate to conductivity which will yield a desired temperature level at some point on the cross section, say, the center $x_1 = 1$, instead of being related to the time parameter τ_1. This relationship can be achieved through the elementary temperature relation (eq. (12)) from which it is seen that, for $x = c/2$,

$$\frac{c^2}{t_m} \frac{q/K}{\left(\bar{U}_{el}\right)_{x=c/2}} = \frac{4}{\tau_1}$$

Accordingly, the results of figure (4) have been replotted in figure (5) in the form of plots of $\frac{\Delta GJ}{\Delta(GJ)_{el}} \equiv \left(\frac{\psi(\tau_1)}{\psi(\tau_1)_{el}}\right)$ against $\frac{c^2}{t_m} \frac{q/K}{\left(\bar{U}_{el}\right)_{x=c/2}}$.

The ordinate $\frac{\Delta GJ}{\Delta(GJ)_{el}}$ is the ratio of the loss of torsional stiffness

calculated with chordwise heat conduction to that calculated without accounting for the influence of chordwise heat conduction. From this figure it is seen that for values of

$$\frac{c^2}{t_m}\frac{q/K}{\left(\bar{U}_{el}\right)_{x=c/2}} < 400$$

torsional stiffness reductions due to a constant uniform heat input q, which are calculated without accounting for the benefits of chordwise heat conduction, will be appreciably in error. The smaller the magnitude of the ratio $\frac{c^2}{t_m}\frac{q/K}{\left(\bar{U}_{el}\right)_{x=c/2}}$, the greater is the effect of chordwise heat conduction on torsional stiffness reductions from this type of heat input. One might infer from this some general principles regarding the reliability of calculations of torsional stiffness which do not account for chordwise heat conduction. For example, if in the laboratory a certain temperature at a point of a given thin wing structure is desired, the magnitude of the heating rate used to reach this temperature must be kept high if calculations of the resulting torsional stiffness, based on the elementary theory, are to be considered reliable. Conversely, for a given fixed heating rate applied to a given structure, calculations of torsional stiffness which neglect chordwise heat conduction can be relied upon only if the temperatures to be achieved in the structure are low.

CONCLUDING REMARKS

Analyses have been made of the effects of chordwise heat conduction on the torsional stiffness reduction of a thin diamond-shaped wing. Analytic solutions for both long- and short-time intervals were obtained by using separation of variables and Mellin transforms. The inclusion of chordwise heat conduction in the temperature distribution analysis produces the greatest effect, as would be expected, in reducing the temperature gradients near the leading and trailing edges of the wing. For a given structure this difference in calculated temperatures near the leading edge is also shown to increase with increasing time. For small time intervals the effect of chordwise heat conduction is small over most of the cross section. For large time intervals the effect of chordwise heat conduction must be taken into account over the whole cross section to obtain satisfactory accuracy.

The inclusion of chordwise heat conduction leads to a finite calculated stiffness reduction whereas the stiffness reduction, calculated

with chordwise heat flow neglected, increases without limit. The effect of chordwise heat conduction on the reduction of torsional stiffness for a diamond-shaped wing subjected to a constant heat input is found to vary inversely as the magnitude of the heating rate and directly as the conductivity of the wing material and the final wing temperatures. If a given diamond-shaped wing is heated at a low heating rate or to a high final wing temperature, the effect of chordwise heat conduction on the calculated torsional stiffness reductions must be considered.

Langley Research Center,
National Aeronautics and Space Administration,
Langley Field, Va., May 8, 1959.

APPENDIX A

DERIVATIONS OF CHORDWISE TEMPERATURE DISTRIBUTION INCLUDING CHORDWISE HEAT FLOW

Bessel Series Solution

As a first step in determining the complete solution to equation (2) for U, consider the quasi-steady-state solution in which transient conditions are neglected. After a long period of time the temperature distribution will stabilize and continued heating of the wedge will only cause a uniform increase in temperature as a linear function of time.

Therefore let

$$U_{qs} = \Phi_1(x_1) + c_1\tau_1 \tag{A1}$$

where c_1 is a constant and $\Phi_1(x_1)$ is some function of x_1.

Substitution of the expression for U_{qs} from equation (A1) into equation (2) and integrating with respect to x_1, using the boundary conditions given by equations (3) and (4) yields

$$U_{qs} = \frac{x_1^2}{2} - x_1 + \tau_1 + c_2 \tag{A2}$$

The constant c_2 can be evaluated by equating the total heat in the double wedge to the heat input over the time τ. In nondimensional form this condition is

$$\int_0^1 x_1 U_{qs}\, dx_1 = \frac{\tau_1}{2} \tag{A3}$$

Thus

$$c_2 = \frac{5}{12}$$

Therefore the quasi-steady-state solution is

$$U_{qs} = \frac{x_1^2}{2} - x_1 + \tau_1 + \frac{5}{12} \tag{A4}$$

The complete temperature distribution analysis including the transient temperature conditions can be written as

$$U = U_{qs} + U_1(x_1,\tau_1) \tag{A5}$$

where $U_1(x_1,\tau_1)$ represents the transient temperature conditions. By substitution of equation (A5) into equation (2) the heat balance equation becomes

$$2x_1\left(\dot{U}_{qs} + \dot{U}_1\right) = 1 + \left(x_1U'_{qs}\right)' + \left(x_1U'\right)' \tag{A6}$$

Substitution of equation (A4) for U_{qs} into equation (A6) yields

$$\dot{U}_1 = \frac{\left(x_1U'_1\right)'}{2x_1} \tag{A7}$$

The boundary conditions on U_1 are the same as those given by equations (3) and (4). However, the initial condition given by equation (5) becomes: $U_1(x_1,0) = -\left(\frac{x_1^2}{2} - x_1 + \frac{5}{12}\right)$. By making use of the method of separation of variables, the solution to equation (A7) can be expressed as

$$U_1 = \left[DJ_0\left(\sqrt{2\lambda}\,x_1\right) + c_3Y_0\left(\sqrt{2\lambda}\,x_1\right)\right]e^{-\lambda\tau_1} \tag{A8}$$

where λ is a positive undetermined constant. Application of the first boundary condition given by equation (3) yields

$$c_3 = 0$$

Application of the second boundary condition given by equation (4) leads to the condition

$$J_1\left(\sqrt{2\lambda}\right) = 0 \tag{A9}$$

which defines values of λ corresponding to the existence of nontrivial solutions of equation (A7). Therefore, the general solution of equation (A7) must have the form

$$U_1 = \sum_{n=0,1,2}^{\infty} D_n J_0(Z_n x_1) e^{\frac{-Z_n^2}{2}\tau_1} \tag{A10}$$

where $Z_n = \sqrt{2\lambda_n}$ is the nth root of equation (A9). By using the initial condition, $U_1(x_1,0) = -\left(\frac{x_1^2}{2} - x_1 + \frac{5}{12}\right)$ and the orthogonality relations for the Bessel function, D_n can be expressed in the form

$$D_n = \frac{\int_0^1 \left(x_1 - \frac{x_1^2}{2} - \frac{5}{12}\right) x_1 J_0(Z_n x_1) dx_1}{\frac{J_0^2}{2}(Z_n)} \tag{A11}$$

Further simplification of the integral in equation (A11), by integration by parts, yields

$$D_n = \frac{-2}{Z_n^2} \frac{\int_0^1 J_0(Z_n x_1) dx_1}{J_0^2(Z_n)} \tag{A12}$$

and

$$D_0 = 0$$

Thus U_1 becomes

$$U_1 = \sum_{n=1,2,3,\ldots}^{\infty} D_n J_0(Z_n x_1) e^{\frac{-Z_n^2}{2}\tau_1} \tag{A13}$$

and the complete expression for U as given by equation (A5) can be written as

$$U = \frac{x_1^2}{2} - x_1 + \tau_1 + \frac{5}{12} + \sum_{n=1,2,3,\ldots}^{\infty} D_n J_0(Z_n x_1) e^{\frac{-Z_n^2}{2}\tau_1} \tag{A14}$$

with D_n defined by equation (A12).

Short-Time Solution

In order to arrive at a short-time solution to equation (2) the temperature distribution of an infinite wedge with apex at $x_1 = 0$ was used to approximate the temperature distribution in the diamond-shaped wing. The character of the problem suggested looking for a solution of the form:

$$U = \varphi_2(\tau_1)\ V\left(\frac{x_1}{\tau_1^n}\right) = \varphi_2(\tau_1)\ V(\xi) \tag{A15}$$

Substitution of equation (A15) into equation (2) yields

$$2x_1 \frac{d\varphi_2(\tau_1)}{d\tau_1} V(\xi) - \frac{2x_1 n}{\tau_1} \xi\varphi_2(\tau_1)\frac{dV(\xi)}{d\xi} = 1 + \frac{\varphi_2(\tau_1)}{\tau^n} \frac{d}{d\xi}\left(\xi \frac{dV(\xi)}{d\xi}\right) \tag{A16}$$

In order to eliminate τ_1 from the coefficients of equation (A16) let $n = 1/2$ and $\varphi_2(\tau_1) = \tau_1^{1/2}$; the result is the ordinary differential equation

$$\xi \frac{d^2V(\xi)}{d\xi^2} + \left(1 + \xi^2\right)\frac{dV(\xi)}{d\xi} - \xi V = -1 \tag{A17}$$

The boundary conditions are

$$\xi \frac{dV(\xi)}{d\xi} \to 0 \qquad (\xi \to 0) \tag{A18}$$

$$V(\xi) \to 0 \qquad (\xi \to \infty) \tag{A19}$$

Note that the initial condition on U is automatically satisfied.

Since $V(\xi)$ is analytic in the interval $0 < \xi < \infty$ and satisfies conditions (A18) and (A19), it has a Mellin transform $f(s)$. (See ref. 5.) Then

$$V(\xi) = \frac{1}{2\pi i} \int_{a-i\infty}^{a+i\infty} f(s)\xi^s\, ds \tag{A20}$$

where a is a real constant yet to be determined. Substitution of this expression for $V(\xi)$ into equation (A17) yields

$$\frac{1}{2\pi i}\int_{a-i\infty}^{a+i\infty}\left[s^2\xi^{s-1} + (s-1)\xi^{s+1}\right]f(s)ds = -1 \qquad \text{(A21)}$$

or

$$\frac{1}{2\pi i}\int_{a-i\infty}^{a+i\infty} s^2 f(s)\xi^{s-1}ds + \frac{1}{2\pi i}\int_{a+2-i\infty}^{a+2+i\infty}(s-3)f(s-2)\,\xi^{s-1}ds = -1 \qquad \text{(A22)}$$

Equation (A22) can be written as

$$\frac{-1}{2\pi i}\oint_{\epsilon} s^2 f(s)\xi^{s-1}ds + \frac{1}{2\pi i}\int_{a+2-i\infty}^{a+2+i\infty}\left[s^2 f(s) + (s-3)f(s-2)\right]\xi^{s-1}ds = -1 \qquad \text{(A23)}$$

where ϵ is the path shown in the following sketch.

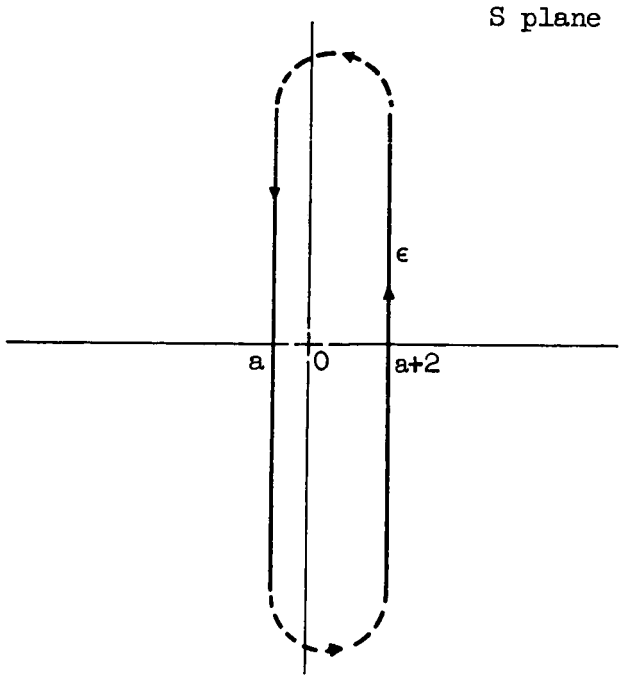

Let

$$s^2 f(s) + (s - 3)f(s - 2) = 0 \tag{A24}$$

Equation (A23) then becomes

$$\frac{1}{2\pi i} \oint_{\epsilon} s^2 f(s) \xi^{s-1} ds = 1 \tag{A25}$$

The general solution to the difference equation (A24) is

$$f(s) = \frac{2^{-s/2} \Gamma\left(\frac{s-1}{2}\right)}{\sin \frac{\pi s}{2} \Gamma^2\left(\frac{s+2}{2}\right)} P(s) \tag{A26}$$

where $P(s) = P(s + 2)$ is an arbitrary function of period two. (See ref. 6, ch. XII.) $P(s)$ and the real number a remain to be determined.

Equation (A25) will be satisfied if the path ϵ encloses the point $s = 1$, $s^2 f(s)$ has a simple pole of residue 1 at $s = 1$ but is otherwise regular inside ϵ, and if all the integrals in question converge. The condition of $V(\xi)$ at infinity (eq. (A19)) will be satisfied if $a < 0$ in equation (A20)). The condition on $V(\xi)$ at zero (eq. (A18)) will be satisfied if $a > 0$ or if $-1 < a < 0$ and if $f(s)$ has at worst a simple pole at $s = 0$ and is otherwise regular for $-1 < a \leqq 0^+$. In addition to these requirements the integral in equation (A20) must, of course, converge. All of these conditions will be met by the following choice for a and $P(s)$.

$$a = -\frac{1}{4} \tag{A27}$$

$$P(s) = \frac{\pi}{4\sqrt{2}} \tag{A28}$$

Thus finally

$$V(\xi) = \frac{1}{2\pi i} \int_{-\frac{1}{4} - i\infty}^{-\frac{1}{4} + i\infty} \frac{\pi}{4\sqrt{2}} \frac{\Gamma\left(\frac{s-1}{2}\right) \xi^s}{2^{s/2} \sin \frac{\pi s}{2} \Gamma^2\left(\frac{s+2}{2}\right)} ds \tag{A29}$$

L
3
4
0

It can be shown rigorously that $V(\xi)$ may be expanded in an asymptotic series of negative powers of ξ by the term-by-term evaluation of the series of residues at the poles to the left of the path of integration of the integrand of equation (A29). Thus

$$V(\xi) \approx \sum_{m=0,1,2,\ldots}^{\infty} R_m(\xi) \tag{A30}$$

where $R_m(\xi)$ is the residue of the integrand at $s = -(2m + 1)$. By making use of the recurrence relations for the gamma function, $\Gamma\left(\frac{s - 1}{2}\right)$ may be expressed as

$$\Gamma\left(\frac{s - 1}{2}\right) = \frac{2}{s - 1}\,\Gamma\left(\frac{s + 1}{2}\right) \tag{A31}$$

and

$$\Gamma\left(\frac{s + 1}{2}\right) = \frac{1}{\frac{s + 1}{2}}\,\Gamma\left(\frac{s + 1}{2} + 1\right) \tag{A32}$$

Hence for $s = -(2m + 1)$

$$\Gamma\left(\frac{s + 1}{2}\right) = \frac{\Gamma\left(\frac{s + 2m + 3}{2}\right) 2^{m+1}}{(s + 1)(s + 3)\ \ldots\ (s + 2m - 1)(s + 2m + 1)} \tag{A33}$$

The sum of the residues of equation (A30) can therefore be written as

$$\frac{\pi}{2\sqrt{2}} \sum_{m=0,1,2,\ldots}^{\infty} \lim_{s \to -(2m + 1)} \frac{\Gamma\left(\frac{s + 2m + 3}{2}\right) \xi^s 2^{m+1}}{2^{s/2} \sin \frac{\pi s}{2} \Gamma\left(\frac{s - 1}{2}\right)(s + 1)(s + 3)\ldots(s + 2m - 1)\Gamma^2\left(\frac{s + 2}{2}\right)} \tag{A34}$$

Let $s = -(2m + 1)$ in equation (A34); thus, the sum of the residues becomes

$$\frac{\pi}{2\sqrt{2}} \sum_{m=0,1,2,\ldots}^{\infty} \frac{\xi^{-2m-1}}{2^{\frac{-2m-1}{2}} (m + 1)m!\Gamma^2\left(\frac{1 - 2m}{2}\right)} \tag{A35}$$

Since $\Gamma\left(\frac{1 - 2m}{2}\right) = \frac{m!\sqrt{\pi}(-1)^m 2^{2m}}{2m!}$ further simplification of equation (A35) results in

$$V(\xi) \approx \sum_{m=0,1,2,\ldots}^{\infty} \frac{[(2m)!]^2}{(m + 1)2^{3m+1}(m!)^3} (\xi)^{-(2m+1)} \tag{A36}$$

Thus the short-time temperature distribution can be written as

$$U \approx \sqrt{\tau_1} \sum_{m=0,1,2,\ldots}^{\infty} \frac{[(2m)!]^2}{2^{3m+1}(m + 1)(m!)^3} \left(\frac{x_1}{\sqrt{\tau_1}}\right)^{-(2m+1)} \tag{A37}$$

The series solution given in equation (A37) for the short-time temperature distribution will rapidly approach its asymptote if $x_1 > \sqrt{\tau_1}$ but becomes impractical as $x_1 \to 0$. In order to calculate the temperature distribution in the vicinity of the leading edge, $x_1 < 0.1$, for short time intervals $V(\xi)$ needs to be expanded in positive powers of ξ. In order to evaluate $V(\xi)$ as a convergent power series in positive powers of ξ, a closed path is chosen to the right of the path of integration in the clockwise direction, and

$$V(\xi) = \frac{1}{2\pi i} \int_{-\frac{1}{4}-i\infty}^{-\frac{1}{4}+i\infty} \frac{\pi}{4\sqrt{2}} \frac{\Gamma\left(\frac{s - 1}{2}\right)\xi^s}{2^{s/2}\sin\frac{\pi s}{2}\,\Gamma^2\left(\frac{s + 2}{2}\right)} ds = - \sum_{m=0,1,2,\ldots}^{\infty} R_m(\xi) \tag{A38}$$

where $R_m(\xi)$ are the residues of the integrand at $s = 0, 1, 2, 4, 6, 8, 10 \ldots$. By making use of the recurrence relation given by equation (A31) for the gamma function, the series of residues of equation (A38) after some simplification become

$$V(\xi) = \sqrt{\frac{\pi}{2}} - \frac{x_1}{\sqrt{\tau_1}} - \sqrt{2\pi} \sum_{n=1,2,3,\ldots}^{\infty} \frac{n(-1)^n(2n-2)!}{2^{3n}(n!)^3} \left(\frac{x_1}{\sqrt{\tau_1}}\right)^{2n} \tag{A39}$$

and

$$U = \sqrt{\frac{\pi}{2}\tau_1} - x_1 - x_1\sqrt{2\pi} \sum_{n=1,2,3,\ldots}^{\infty} \frac{n(-1)^n(2n-2)!}{2^{3n}(n!)^3} \left(\frac{x_1}{\sqrt{\tau_1}}\right)^{2n-1} \tag{A40}$$

As a further check on the validity of the resulting series solutions given by equations (A36) and (A39), the solutions were substituted back into the ordinary differential equation (A17) and satisfied it exactly.

APPENDIX B

EVALUATION OF THE INTEGRALS IN THE SHORT-TIME SOLUTION FOR TORSIONAL STIFFNESS REDUCTION

$$\int_0^1 x_1^j V\left(\frac{x_1}{\sqrt{\tau_1}}\right)dx_1 = \frac{\tau_1^{\frac{j+1}{2}}}{2\pi i}\int_{-\frac{1}{4}-i\infty}^{-\frac{1}{4}+i\infty}\int_0^{\frac{1}{\sqrt{\tau_1}}} f(s)\xi^{s+j}d\xi\,ds \qquad (j = 1, 2, 3, \ldots) \quad \text{(B1)}$$

L 3 4 0

Since the real part of the exponent of ξ is always positive under the integral sign, the contribution of the lower limit (zero) is null. Therefore,

$$\int_0^1 x_1^j V\left(\frac{x_1}{\sqrt{\tau_1}}\right)dx_1 = \frac{\tau_1^{\frac{j+1}{2}}}{2\pi i}\int_{-\frac{1}{4}-i\infty}^{-\frac{1}{4}+i\infty} \frac{f(s)\left(\frac{1}{\sqrt{\tau_1}}\right)^{s+(j+1)}}{s+(j+1)}\,ds \qquad (j = 1, 2, 3, \ldots) \quad \text{(B2)}$$

For the short-time solution $\frac{1}{\sqrt{\tau_1}} \gg 1$ it is appropriate for computational purposes to expand the integrals in equation (B2) in an asymptotic series of negative powers of $\frac{1}{\sqrt{\tau_1}}$. Thus

$$\int_0^1 x_1 V\left(\frac{x_1}{\sqrt{\tau_1}}\right)dx_1 \approx \sum_{m=0,1,2,\ldots}^{\infty} R_m\left(\frac{1}{\sqrt{\tau_1}}\right) \qquad \text{(B3)}$$

where $R_m\left(\frac{1}{\sqrt{\tau_1}}\right)$ is the residue of the integrand at $s = -(2m + 1)$. By making use of the recurrence relations for the gamma functions as was

done in appendix A, the evaluation of the series of residues after some simplification can be written as

$$\int_0^1 x_1 V\left(\frac{x_1}{\sqrt{\tau_1}}\right)dx_1 \approx \sum_{n=0,1,2,\ldots}^{\infty} \frac{\left[(2n)!\right]^2 \tau_1^{n+1/2}}{(1 - 2n^2 - n)2^{3n+1} n!} \tag{B4}$$

Similarly, the asymptotic series for $\int_0^1 x_1^2 V\left(\frac{x_1}{\sqrt{\tau_1}}\right)dx_1$ is the series of residues at $s = -(2m + 1)$. However, the integrand possesses a double pole at $s = -3$ as can be seen from

$$\int_0^1 x_1^2 V\left(\frac{x_1}{\sqrt{\tau_1}}\right)dx_1 = \frac{\tau^{3/2}}{2\pi i} \int_{-\frac{1}{4}-i\infty}^{-\frac{1}{4}+i\infty} \frac{\pi}{4\sqrt{2}} \frac{\Gamma\left(\frac{s-1}{2}\right)\left(\frac{1}{\sqrt{\tau_1}}\right)^{s+3}}{2^{s/2}(s+3)\sin\frac{\pi s}{2}\,\Gamma^2\left(\frac{s+2}{2}\right)} ds \tag{B5}$$

and equations (A31) and (A33). By making use of residue theory and the recurrence relations for the gamma function, the series of residues of equation (B5) after some simplification can be written as

$$\int_0^1 x_1^2 V\left(\frac{x_1}{\sqrt{\tau_1}}\right)dx_1 \approx \frac{\sqrt{\tau_1}}{4} - \frac{5}{32}\tau_1\sqrt{\tau_1} + \frac{\tau_1\sqrt{\tau_1}}{16}\gamma + \frac{3}{16}\tau_1\sqrt{\tau_1}\log_e 2 + \frac{\tau_1\sqrt{\tau_1}}{8}\log_e\frac{1}{\sqrt{\tau_1}} + \sum_{n=2,3,4,\ldots}^{\infty} \frac{\left[(2n)!\right]^2 \tau_1^{n+1/2}}{2^{3n+2}(1 - n^2)(n!)^3} \tag{B6}$$

where $\gamma = 0.5772157\ldots$ Euler's constant. The evaluation of the asymptotic series for $\int_0^1 x_1^3 V\left(\frac{x_1}{\sqrt{\tau_1}}\right)dx_1$ can also be found as the series of residues at $s = -(2m + 1)$. The integrand possesses all simple poles at $s = -(2m + 1)$ as can be seen from

$$\int_0^1 x_1^3 V\left(\frac{x_1}{\sqrt{\tau_1}}\right) dx_1 = \frac{\tau_1^2}{2\pi i} \int_{-\frac{1}{4}-i\infty}^{-\frac{1}{4}+i\infty} \frac{\pi}{2\sqrt{2}} \frac{1}{s-1} \frac{1}{s+4} \frac{\Gamma\left(\frac{s+1}{2}\right)\left(\frac{1}{\sqrt{\tau_1}}\right)^{s+4}}{2^{s/2} \sin\frac{\pi s}{2}\, \Gamma^2\left(\frac{s+2}{2}\right)} ds \tag{B7}$$

The solution for the series of residues is similar to the solutions previously arrived at and the resulting expression is

$$\int_0^1 x_1^3 V\left(\frac{x_1}{\sqrt{\tau_1}}\right) dx_1 \approx \sum_{n=0,1,2,\ldots}^{\infty} \frac{\left[(2n)!\right]^2 \tau_1^{n+1/2}}{(3 - 2n^2 + n) 2^{3n+1} (n!)^3} \tag{B8}$$

L
3
4
0

APPENDIX C

EVALUATION OF THE INTEGRAL $\int_0^1 J_0(Z_n x_1)\,dx_1$

Substitution in a known identity (see ref. 7) for $\int_0^Z J_0(Z)dZ$ results in

$$\int_0^1 J_0(Z_n x_1)\,dx_1 = \left\{ J_0(Z_n) + \frac{\pi}{2}\left[J_1(Z_n)\boldsymbol{\mathcal{S}}_0(Z_n) - J_0(Z_n)\boldsymbol{\mathcal{S}}_1(Z_n)\right]\right\} \qquad (C1)$$

where $\boldsymbol{\mathcal{S}}_n(Z_n)$ is the Struve function of order n. Since $J_1(Z_n) = 0$, equation (C1) reduces to

$$\int_0^1 J_0(Z_n x_1)\,dx_1 = J_0(Z_n) - \frac{\pi}{2} J_0(Z_n)\boldsymbol{\mathcal{S}}_1(Z_n) \qquad (C2)$$

For values of $0 < Z_n < 15.9$, tabulated values of $J_0(Z_n)$ and $\boldsymbol{\mathcal{S}}_1(Z_n)$ are given in reference 8. When $Z_n > 15.9$ (see ref. 7)

$$\boldsymbol{\mathcal{S}}_1(Z_n) \approx Y_1(Z_n) + \frac{2}{\pi} + \frac{2}{\pi Z_n^2} \qquad (C3)$$

Therefore equation (C2) becomes

$$\int_0^1 J_0(Z_n x_1)\,dx_1 = -\frac{\pi}{2}\left[J_0(Z_n)Y_1(Z_n) + \frac{2}{\pi Z_n^2} J_0(Z_n)\right] \quad (Z_n > 15.9) \qquad (C4)$$

A known identity involving the Bessel functions of the first and second kind (ref. 8) is

$$Y_0(Z_n)J_1(Z_n) - Y_1(Z_n)J_0(Z_n) = \frac{2}{\pi Z_n} \tag{C5}$$

and since $J_1(Z_n) = 0$, equation (C4) becomes

$$\int_0^1 J_0(Z_n x_1)dx_1 = \frac{1}{Z_n}\left[1 - \frac{J_0(Z_n)}{Z_n}\right] \quad (Z_n > 15.9) \tag{C6}$$

L
3
4
0

The asymptotic approximation for $J_0(Z_n)$ is

$$J_0(Z_n) \approx \sqrt{\frac{2}{\pi Z_n}}\left[\sin\left(Z_n + \frac{\pi}{4}\right) + \frac{1}{8Z_n}\sin\left(Z_n - \frac{\pi}{4}\right)\right] \tag{C7}$$

REFERENCES

1. Budiansky, Bernard, and Mayers, J.: Influence of Aerodynamic Heating on the Effective Torsional Stiffness of Thin Wings. Jour. Aero. Sci., vol. 23, no. 12, Dec. 1956, pp. 1081-1093, 1108.

2. Bryson, A. E., Budiansky, Bernard, and Carrier, George F.: Leading-Edge Temperature of a Flat Plate Subjected to Aerodynamic Heating. Jour. Aero. Sci. (Readers' Forum), vol. 24, no. 4, Apr. 1957, pp. 311-312.

3. Mirsky, I.: Temperature Distribution in a Diamond-Shaped Model Wing with Constant Heat Input. PIBAL Rep. No. 228 (Contract AF 33(616)-116), Polytechnic Inst. Brooklyn, July 1953.

4. Timoshenko, S., and Goodier, J. N.: Theory of Elasticity. Second ed., McGraw-Hill Book Co., Inc., 1951.

5. Tranter, C. J.: Integral Transforms in Mathematical Physics. John Wiley & Sons, Inc., 1951.

6. Milne-Thomson, L. M.: The Calculus of Finite Differences. MacMillan and Co., Ltd., 1933.

7. McLachlan, N. W.: Bessel Functions for Engineers. Clarendon Press (Oxford), 1934.

8. Jahnke, Eugene, and Emde, Fritz: Table of Functions With Formulae and Curves. Rev. ed., Dover Publications, 1943.

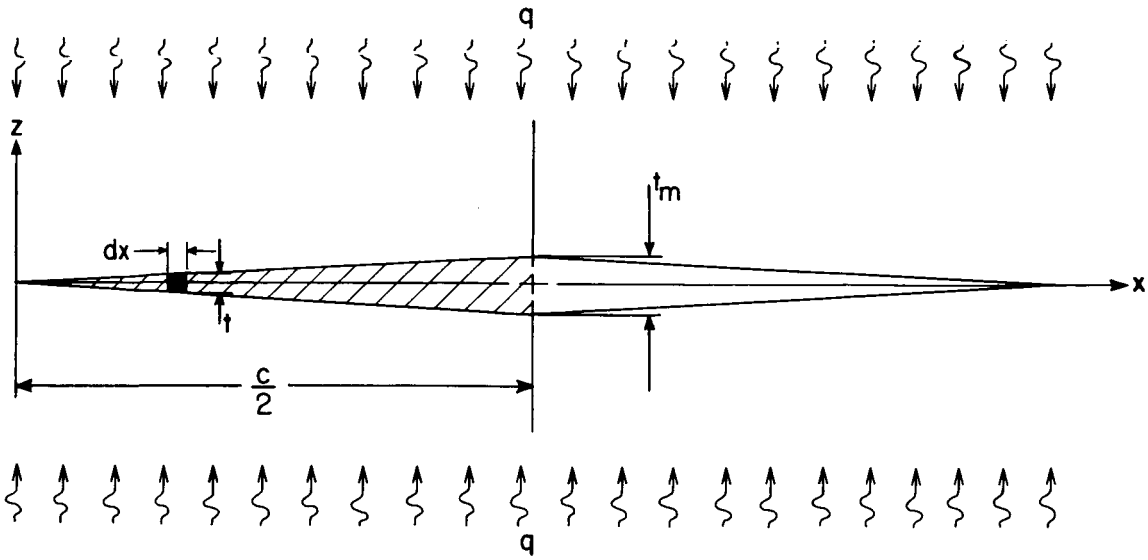

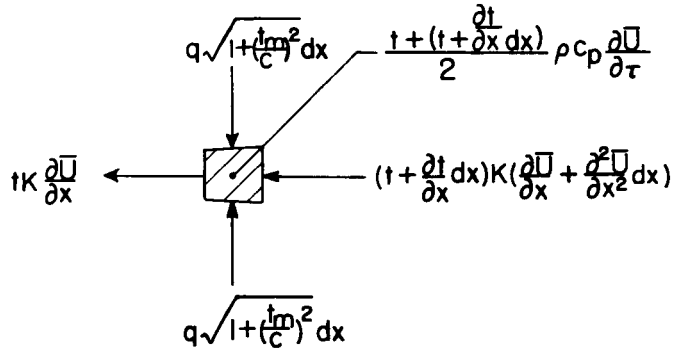

Element

Figure 1.- Diamond-shaped wing under a constant heat input.

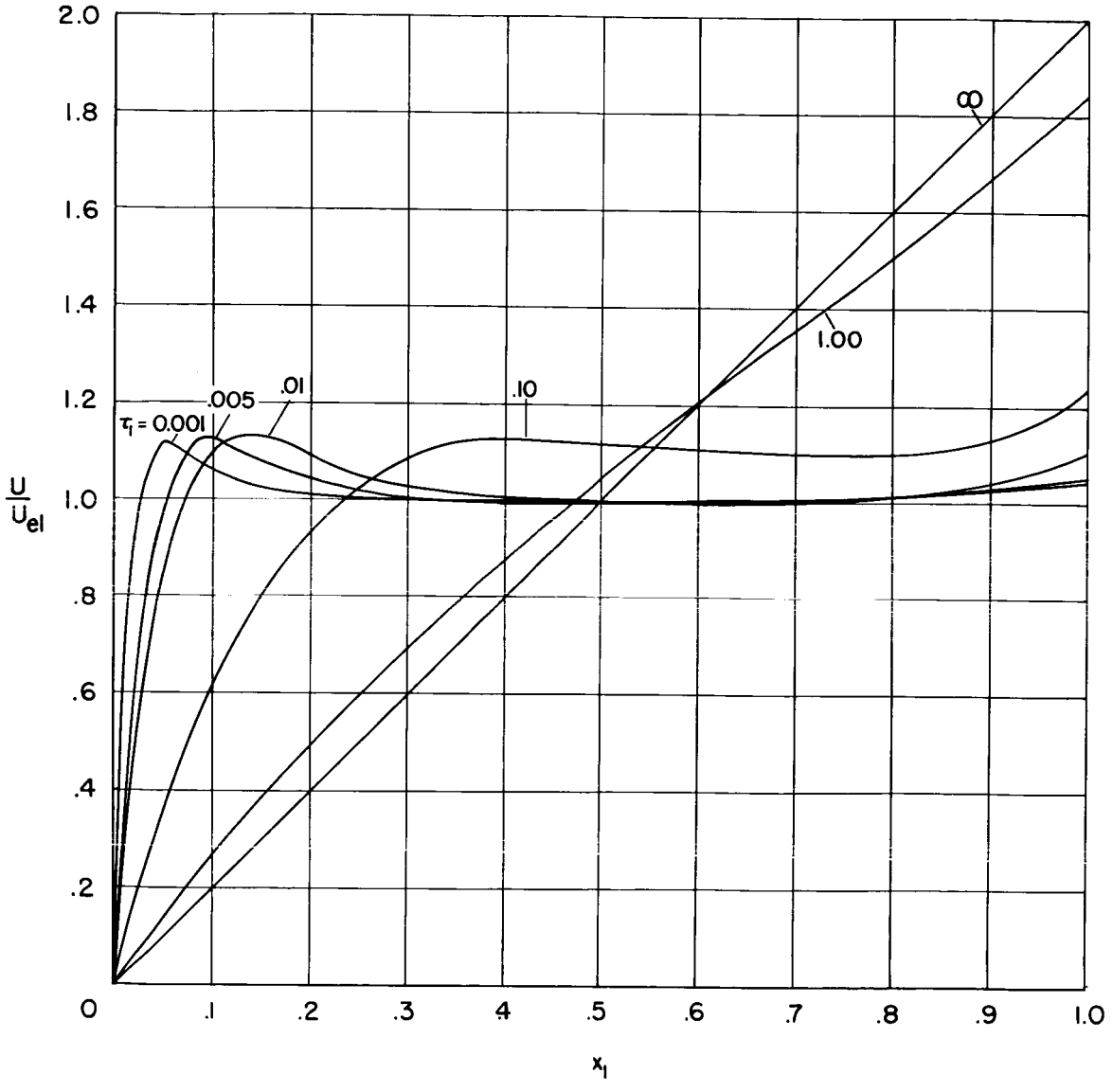

Figure 2.- Ratio of temperature calculated with and without chordwise heat conduction plotted across the half-chord for various values of the time parameter $\tau_1 = \frac{8\eta}{c^2}\tau$.

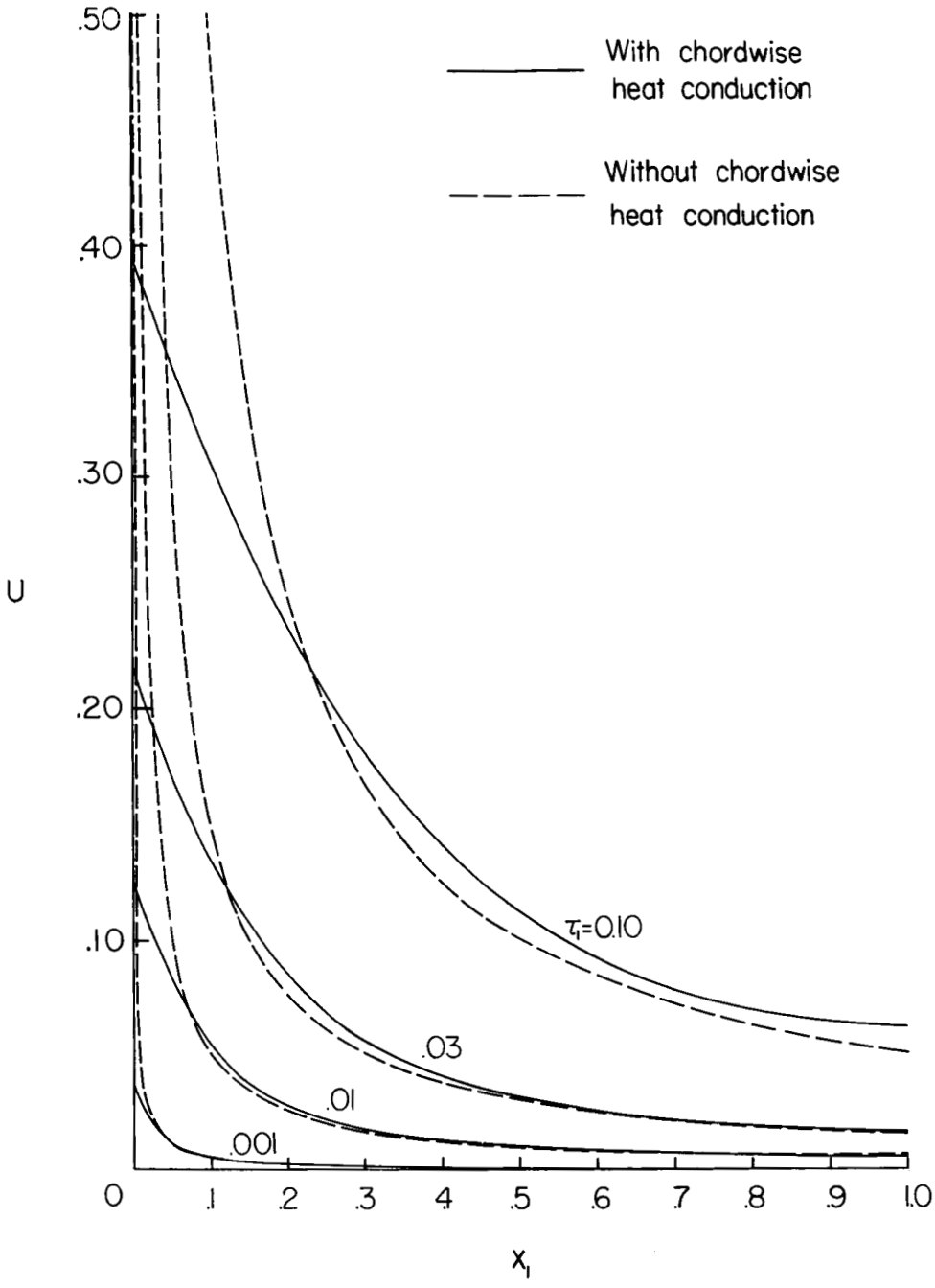

Figure 3.- Temperature distribution calculated with and without chordwise heat conduction plotted across the half-chord for various values of the time parameter $\tau_1 = \frac{8\eta}{c^2}\tau$.

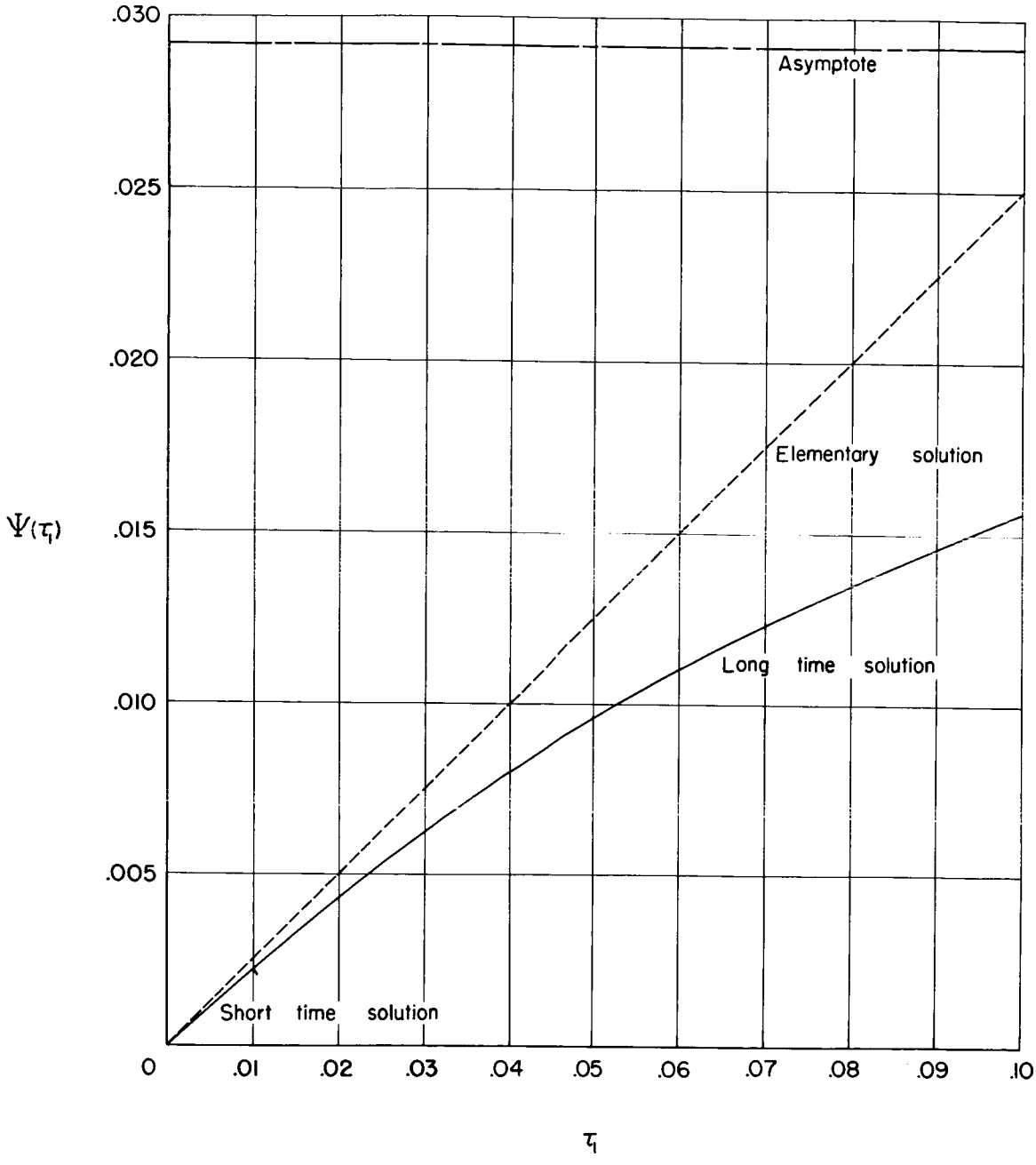

Figure 4.- Parameter $\Psi(\tau_1)$ as a function of the time parameter $\tau_1 = \frac{8\eta}{c^2}\tau$.

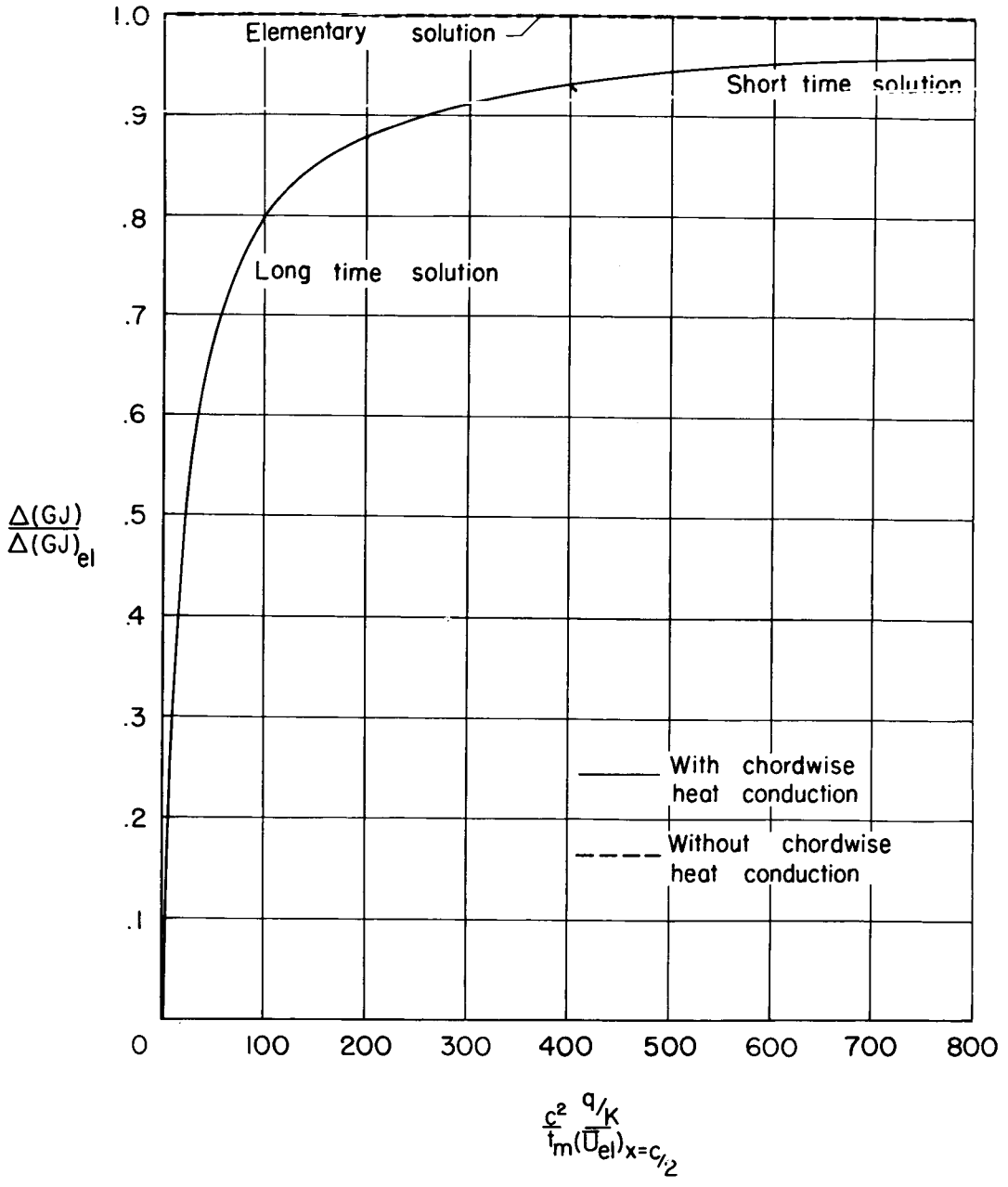

Figure 5.- The ratio of the percent change in torsional stiffness calculated with and without chordwise heat conduction as a function of the heating rate, conductivity, and temperature at the midchord $\frac{c^2}{t_m}\frac{q/K}{(\bar{U}_{el})_{x=c/2}}$.